An analytic functional form for characterization and generation of axisymmetric plasma boundaries

2013 Plasma Phys. Control. Fusion 55 095009

(http://iopscience.iop.org/0741-3335/55/9/095009)

IOP Publishing Plasma Physics and Controlled Fusion
Plasma Phys. Control. Fusion **57** (2015) 049501 (1pp) doi:10.1088/0741-3335/57/4/049501

Corrigendum: An analytic functional form for characterization and generation of axisymmetric plasma boundaries (2013 *Plasma Phys. Control. Fusion* **55** 095009)

T C Luce

General Atomics, PO Box 85608, San Diego, CA 92186–5608, USA

E-mail: luce@fusion.gat.com

Received 15 January 2015, revised 2 February 2015
Accepted for publication 6 February 2015
Published 25 February 2015

In the translation of the derived equations to table form, several errors were introduced by the author in table 4. The equations for X in quadrants I and IV should have a minus sign rather than a plus sign, and in quadrant III there is an extraneous 'a' at the end of the formula. The equations for the ζ-point constraint and the x-point constraint in quadrants II and III should have a minus sign preceding δ_u and δ_l, respectively. To aid the readers, the corrected table is given below. Tables 1 and 3 were corrected in a previous corrigendum [1]. The author gratefully acknowledges Mr A Garbo of the Georgia Institute of Technology for initiating the dialogue leading to the correction of these errors.

Reference

[1] Luce T C 2013 *Plasma Phys. Control. Fusion* **55** 119501

Table 4. New variables and constraints for each quadrant for x-point plasmas.

Quadrant	X	x-point constraint	ζ-point constraint	x-point slope constraint
I	$R - a(1/\varepsilon - 1) - \alpha$	$[1 - a/\alpha(1+\delta_u)]^n + (\kappa_u a/\beta)^n - 1$	$[1 + a(1+\delta_u)(1-1/\sqrt{2})(\zeta_{uo}-1)/a]^n + (\kappa_u a[1/\sqrt{2} + \zeta_{uo}(1-1/\sqrt{2})]/\beta)^n = 1$	$\beta([\alpha - a(1+\delta_u)]/\kappa_u a)^{n-1} \times (\beta/\alpha)^{n-1} = \begin{cases} 1-\delta_u & \delta_u \geq 0 \\ 1/(1+\delta_u) & \delta_u < 0 \end{cases}$
II	$a(1/\varepsilon - 1) + \alpha - R$	$[1 - a/\alpha(1-\delta_u)]^n + (\kappa_u a/\beta)^n - 1$	$[1 + a(1-\delta_u)(1-1/\sqrt{2})(\zeta_{ui}-1)/a]^n + (\kappa_u a[1/\sqrt{2} + \zeta_{ui}(1-1/\sqrt{2})]/\beta)^n = 1$	$\beta([\alpha - a(1-\delta_u)]/\kappa_u a)^{n-1} \times (\beta/\alpha)^{n-1} = \begin{cases} 1/(1-\delta_u) & \delta_u \geq 1 \\ 1+\delta_u & \delta_u < 0 \end{cases}$
III	$a(1/\varepsilon - 1) + \alpha - R$	$[1 - a/\alpha(1-\delta_l)]^n + (\kappa_l a/\beta)^n = 1$	$[1 + a(1-\delta_l)(1-1/\sqrt{2})(\zeta_{li}-1)/a]^n + (\kappa_l a[1/\sqrt{2} + \zeta_{li}(1-1/\sqrt{2})]/\beta)^n = 1$	$\beta([\alpha - a(1-\delta_l)]/\kappa_l a)^{n-1} \times (\beta/\alpha)^{n-1} = \begin{cases} 1/(1-\delta_l) & \delta_l \geq 0 \\ 1+\delta_l & \delta_l < 0 \end{cases}$
IV	$R - a(1/\varepsilon - 1) - \alpha$	$[1 - a/\alpha(1+\delta_l)]^n + (\kappa_l a/\beta)^n = 1$	$[1 + a(1+\delta_l)(1-1/\sqrt{2})(\zeta_{lo}-1)/a]^n + (\kappa_l a[1/\sqrt{2} + \zeta_{lo}(1-1/\sqrt{2})]/\beta)^n = 1$	$\beta([\alpha - a(1+\delta_l)]/\kappa_l a)^{n-1} \times (\beta/\alpha)^{n-1} = \begin{cases} 1-\delta_l & \delta_l \geq 0 \\ 1/(1+\delta_l) & \delta_l < 0 \end{cases}$

Plasma Phys. Control. Fusion **55** (2013) 119501 (1pp) doi:10.1088/0741-3335/55/11/119501

Corrigendum: An analytic functional form for characterization and generation of axisymmetric plasma boundaries

2013 *Plasma Phys. Control. Fusion* **55** 095009

T C Luce

General Atomics, PO Box 85608, San Diego, CA 92186-5608, USA

Received 21 August 2013
Published 18 October 2013
Online at stacks.iop.org/PPCF/55/119501

In the translation of the derived equations to table form, several errors were introduced by the author in tables 1 and 3. In table 1, the references to $R_{z_{\max}}$ in quadrants III and IV should be to $R_{z_{\min}}$. In table 3, the equations for x in quadrants I and IV should have a minus sign rather than a plus sign, and the definition of n in quadrant III should have ζ_{li} rather than ζ_{u}. To aid the readers, the corrected tables are given below. The author gratefully acknowledges Dr M Bongard of University of Wisconsin-Madison for bringing these errors to his attention.

Table 1. Definitions of the parameters for generating reference ellipses by equation (10) for the four quadrants. Note that x and y are defined as positive definite in each quadrant, which is the equivalent of reflecting the curve in all quadrants into quadrant I. This is necessary for the analytic forms introduced later where x and y will have non-integer exponents.

Quadrant		x	y	A	B
I	Upper outer	$R - R_{z_{\max}}$	$z - z_{R_{\max}}$	$R_{\max} - R_{z_{\max}}$	$z_{\max} - z_{R_{\max}}$
II	Upper inner	$R_{z_{\max}} - R$	$z - z_{R_{\max}}$	$R_{z_{\max}} - R_{\min}$	$z_{\max} - z_{R_{\max}}$
III	Lower inner	$R_{z_{\min}} - R$	$z_{R_{\max}} - z$	$R_{z_{\min}} - R_{\min}$	$z_{R_{\max}} - z_{\min}$
IV	Lower outer	$R - R_{z_{\min}}$	$z_{R_{\max}} - z$	$R_{\max} - R_{z_{\min}}$	$z_{R_{\max}} - z_{\min}$

Table 3. Values of the superellipse parameters in each quadrant in terms of the dimensionless geometric parameters.

Quadrant	x	y	A	B	n
I	$R - a(1/\varepsilon - \delta_{\mathrm{u}})$	$z - z_{\mathrm{off}}$	$a(1 + \delta_{\mathrm{u}})$	$\kappa_{\mathrm{u}} a$	$-\ln(2)/\ln[1/\sqrt{2} + \zeta_{\mathrm{uo}}(1 - 1/\sqrt{2})]$
II	$a(1/\varepsilon - \delta_{\mathrm{u}}) - R$	$z - z_{\mathrm{off}}$	$a(1 - \delta_{\mathrm{u}})$	$\kappa_{\mathrm{u}} a$	$-\ln(2)/\ln[1/\sqrt{2} + \zeta_{\mathrm{ui}}(1 - 1/\sqrt{2})]$
III	$a(1/\varepsilon - \delta_{l}) - R$	$z_{\mathrm{off}} - z$	$a(1 - \delta_{1})$	$\kappa_{\mathrm{l}} a$	$-\ln(2)/\ln[1/\sqrt{2} + \zeta_{\mathrm{li}}(1 - 1/\sqrt{2})]$
IV	$R - a(1/\varepsilon - \delta_{l})$	$z_{\mathrm{off}} - z$	$a(1 + \delta_{1})$	$\kappa_{l} a$	$-\ln(2)/\ln[1/\sqrt{2} + \zeta_{\mathrm{lo}}(1 - 1/\sqrt{2})]$

Plasma Phys. Control. Fusion **55** (2013) 095009 (7pp) doi:10.1088/0741-3335/55/9/095009

An analytic functional form for characterization and generation of axisymmetric plasma boundaries

T C Luce

General Atomics, PO Box 85608, San Diego, CA 92186-5608, USA

Received 30 April 2013, in final form 12 June 2013
Published 16 July 2013
Online at stacks.iop.org/PPCF/55/095009

Abstract
An analytic form to describe the boundary of an axisymmetric plasma is proposed. This new form uses a generalization of the family of superellipses. The plasma boundaries of existing tokamaks are well described using the compact notation. The form employs eleven parameters of which five are standard, two are generalizations of a standard parameter and four are introduced here. With these same parameters, a closed-form analytic solution can be used to generate new boundaries without x-points. If the desired boundary has x-points, the analytic form can be extended in a manner for which a closed-form solution has not been found, but does have an exact solution that can be found numerically. This new form should be useful for variety of physics studies that use magnetohydrodynamic equilibria, such as the dependence of plasma stability on shape and design of poloidal field coil sets that can support a defined range of shapes.

1. Introduction

The utility of a compact characterization of the geometric shape of an axisymmetric toroidal plasma is generally acknowledged. Confinement scalings that are used to project fusion gain in burning plasmas in tokamaks employ basic shaping parameters as variables [1, 2]. The magnetohydrodynamic (MHD) stability of tokamak plasmas has been cast in terms of similar geometric parameters, but generally a larger number of parameters are used [3, 4]. The design of the poloidal field coil systems for fusion experiments requires the means to generate the boundary condition for the equilibrium solver, including the possibility of x-points (e.g. [5, 6]). Given this long history of the need to generate a boundary or characterizing the geometry of the plasma by a small number of parameters, it is somewhat surprising that a standard functional form for such applications that includes the possibility of x-points does not exist in the literature. As will be shown here, a rather simple functional form provides the means to characterize or generate the boundaries of many of the axisymmetric plasmas of interest today.

2. Definition of shape parameters

The definitions of the basic geometric parameters for describing the plasma shape have been standardized for many years. In order to illustrate the geometric parameters, figure 1 shows two examples of boundaries from plasmas formed in the DIII-D tokamak [7] inferred using the EFIT equilibrium reconstruction code [8]. On the left side, a plasma without x-points is shown, while on the right is a plasma with x-points at the top and bottom. Neither plasma is symmetric about any horizontal line, which is important to accommodate in the forms introduced here, in order to generate and characterize plasma boundaries with a single x-point (either top or bottom). Each of these plasmas is assumed to be axisymmetric about the dashed vertical line.

The basic geometric parameters are defined in terms of the points shown in figure 1, namely the maxima and minima in radius and elevation. From these points, the following definitions are made:

$$\text{Major radius } R_{\text{geo}} \equiv (R_{\max} + R_{\min})/2 \tag{1}$$

$$\text{Minor radius } a \equiv (R_{\max} - R_{\min})/2 \tag{2}$$

$$\text{Inverse aspect ratio } \varepsilon \equiv a/R_{\text{geo}} \tag{3}$$

$$\text{Elongation } \kappa \equiv (z_{\max} - z_{\min})/2a \tag{4}$$

$$\text{Upper triangularity } \delta_{\text{u}} \equiv (R_{\text{geo}} - R_{z_{\max}})/a \tag{5}$$

$$\text{Lower triangularity } \delta_{\text{l}} \equiv (R_{\text{geo}} - R_{z_{\min}})/a. \tag{6}$$

These definitions and nomenclature are standard.

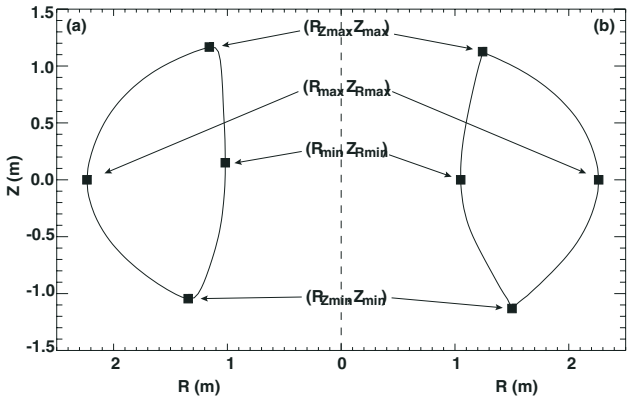

Figure 1. Contours of the last closed flux surfaces for two DIII-D plasmas as reconstructed from magnetics data: (*a*) limited plasma (#146478 at 5010 ms), (*b*) double-null plasma (#120343 at 3000 ms). Note that the plasma boundary in (*a*) has been reflected from the standard point of view to keep the axis of symmetry the same for both boundaries. The filled squares denote the four extremal points used as reference locations as described in the text.

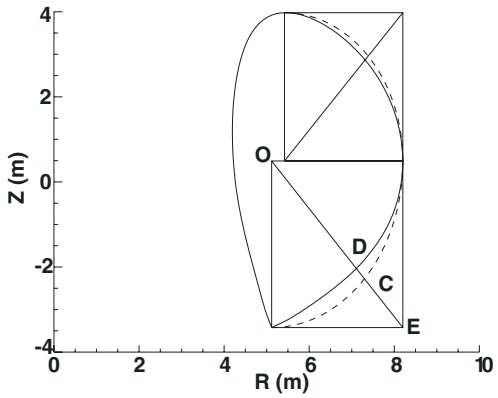

Figure 2. Contour of the ITER last closed flux surface from the 2008 ITER Baseline Design. The reference frames for the squareness calculations for the upper and lower outer quadrants (I and IV, respectively) are shown. The reference ellipses for these quadrants as defined in the text are shown in dashed lines.

In addition to these standard parameters, it is necessary to define a few new parameters to characterize the plasma shape as required for the purposes discussed here. The first new parameters are a straightforward extension of the elongation defined in equation (4):

$$\text{Upper elongation } \kappa_u \equiv (z_{max} - z_{off})/a \tag{7}$$

$$\text{Lower elongation } \kappa_l \equiv (z_{off} - z_{min})/a, \tag{8}$$

where

$$z_{off} \equiv z_{R_{max}}. \tag{9}$$

The need for this will be clearer when the mathematical form for the boundary is introduced in the following section, but it is clear from inspection of typical plasmas with a single x-point at either the top or bottom that the elongation of the upper and lower portion of the plasma need not be the same. The offset of the plasma along the axis of symmetry z_{off} is referenced to the height of the maximum radius R_{max}. Note that the height of the minimum major radius is not necessarily the same as z_{off} (see the plasma on the left of figure 1). In the form of the boundary shape introduced here, this possibility is ignored, but can be accounted for by defining a separate elongation for each quadrant of the plasma.

The second new set of parameters consists of a measure of curvature of the boundary between the four extremal points shown in figure 1. This measure will be called the squareness, for reasons that will become clearer in a moment. The reference chosen here for the squareness is an ellipse that connects one of the elevation extrema to one of the radius extrema (dashed lines in figure 2). This curve can be written in the standard analytic form:

$$x^2/A^2 + y^2/B^2 = 1, \tag{10}$$

with the definitions in each of the four quadrants given in table 1. The second reference line required is the diagonal bisecting the quadrant bounding box as shown in figure 2. In the lower outer quadrant box, this is the line segment OE shown in the figure. Similar quadrant bounding boxes for the inner quadrants exist, but are not shown in figure 2. The point C is the intersection point of the line bisecting the quadrant with the reference ellipse, while point D is the intersection point of the line and the actual (or desired) boundary. The squareness can now be defined as:

$$\zeta_{1o} \equiv (L_{OD} - L_{OC})/L_{CE}, \tag{11}$$

where L is the length of the line segment connecting the two points in the subscript. Here the initial subscript indicates whether the squareness refers to the upper (u) or lower (l) part of the plasma boundary and the second subscript indicates whether the squareness refers to the inner (i) or outer (o) part of the plasma boundary. It is now possible to give an intuitive motivation for naming this parameter 'squareness'. For $\zeta \to 1$, the plasma boundary will conform to the quadrant bounding box and have a 'square' corner, while $\zeta = 0$ corresponds exactly to an ellipse. Plasmas with positive ζ are 'more square' than an ellipse; conversely a negative value of ζ means the shape is 'less square' (or has 'lower squareness') than an ellipse.

Other parameterizations have been proposed previously to incorporate similar characterization of the boundary shape between the extrema used to define the standard shape parameters. Pomphrey *et al* adopted an approach related to a multipole expansion by introducing a boundary with a cos 4θ term, where θ is the poloidal angle [9]. As shown in their figure 5, an equally spaced set of eight poloidal field coils at constant distance from the center of the plasma could generate a square plasma, i.e. one with maximum radii spaced by $\pi/2$ in angle. Multipole expansions to describe the types of plasma boundaries typical of modern tokamaks are not very efficient (i.e. many higher order moments are needed), especially for boundaries with x-points and up–down asymmetry. An analytic form attributed to Miller was used by Turnbull *et al* to examine the variation of MHD stability with shape [4]:

$$r(\theta) = R_0 + a\cos[\theta + \sin^{-1}(\delta \sin\theta)], \tag{12}$$

$$z(\theta) = z_0 + \kappa a \sin(\theta + \zeta \sin 2\theta), \tag{13}$$

Table 1. Definitions of the parameters for generating reference ellipses by equation (10) for the four quadrants. Note that x and y are defined as positive definite in each quadrant, which is the equivalent of reflecting the curve in all quadrants into quadrant I. This is necessary for the analytic forms introduced later where x and y will have non-integer exponents.

Quadrant		x	y	A	B
I	Upper outer	$R - R_{z_{\max}}$	$z - z_{R_{\max}}$	$R_{\max} - R_{z_{\max}}$	$z_{\max} - z_{R_{\max}}$
II	Upper inner	$R_{z_{\max}} - R$	$z - z_{R_{\max}}$	$R_{z_{\max}} - R_{\min}$	$z_{\max} - z_{R_{\max}}$
III	Lower inner	$R_{z_{\max}} - R$	$z_{R_{\max}} - z$	$R_{z_{\max}} - R_{\min}$	$z_{R_{\max}} - z_{\min}$
IV	Lower outer	$R - R_{z_{\min}}$	$z_{R_{\max}} - z$	$R_{\max} - R_{z_{\max}}$	$z_{R_{\max}} - z_{\min}$

Table 2. Evaluation of extrema locations and shape parameters defined in the text for the plasma boundaries illustrated in figures 1 and 2.

Parameter	Figure 1(a)	Figure 1(b)	Figure 2
$R_{\max}$, $z_{R_{\max}}$	2.234, 0.000	2.263, 0.000	8.201, 0.493
$R_{z_{\max}}$, $z_{\max}$	1.159, 1.167	1.243, 1.126	5.420, 3.978
$R_{\min}$, $z_{R_{\min}}$	1.019, 0.150	1.050, 0.000	4.194, 1.176
$R_{z_{\min}}$, $z_{\min}$	1.345, −1.045	1.501, −1.132	5.117, −3.424
R_{geo}	1.626	1.657	6.204
a	0.608	0.606	1.998
ε	0.374	0.366	0.322
κ	1.821	1.862	1.847
κ_{u}	1.920	1.857	1.745
κ_{l}	1.719	1.866	1.961
δ_{u}	0.769	0.682	0.393
δ_{l}	0.463	0.256	0.544
ζ_{uo}	−0.155	−0.207	−0.090
ζ_{ui}	0.255	−0.414	0.199
ζ_{li}	−0.174	−0.426	−0.488
ζ_{lo}	−0.227	−0.333	−0.210
z_{off}	0.000	0.000	0.493

where θ is again the poloidal angle, R_0 corresponds to equation (1), z_0 to equation (9), a to equation (2), κ to equation (4) and δ to equation (5) but assuming up–down symmetry. (Up–down or even in–out symmetry is not required by this formulation, but is assumed here for brevity of discussion.) The parameter ζ is called the squareness, and figure 1 of [4] shows how the boundary shape changes as a function of ζ. This analytic form is quite useful for generating boundaries for stability calculations without considering an x-point, but it permits no clear extension to describe a boundary with an x-point. Recently, Cerfon and Freidberg introduced a means for introducing an x-point in this form when the plasma equilibrium is in the Solov'ev form [10]. The variation corresponding to squareness here is described in terms the curvature of the boundary at the extrema. To introduce an x-point, the curvature constraints at the extrema where an x-point is desired are replaced with derivative constraints to describe a null in the poloidal magnetic field, but in a manner requiring knowledge of the variation of the poloidal flux in space. This form is quite elegant and powerful for the problem addressed in [10], but for the problems of interest here, characterizing a potential boundary shape or setting a target shape for generating coil currents, a solution for or parameterization of the poloidal flux may not be available. Another empirical definition of squareness has been introduced [11], based on the form used in the DIII-D Plasma Control System. Rather than an ellipse connecting neighboring extrema as the reference curve, that definition used a straight line as the reference curve. This definition yields squareness that is always positive and is marginally simpler to implement mathematically. However, it has the aesthetically displeasing consequence that circular plasmas have finite squareness and diamond-shaped plasmas (in principle) have zero squareness, despite being a square rotated by $\pi/4$. The slight increase in complexity of the form adopted here over that in [11] seems warranted by the added intuitive benefits (the sign of ζ gives immediately a comparison to an ellipse) and the closer relation to the squareness familiar to the theory community defined in equation (13).

The shape parameters can now be computed for the two boundaries shown in figure 1 and the boundary shown in figure 2. The values for the parameters defined in equations (1) through (9) and the four values of squareness defined by analogy with equation (11) are given in table 2. These re-emphasize some of the points mentioned above. For example, κ_{u} and κ_{l} can be the same as the standard definition of κ, but need not be. The values of $z_{R_{\min}}$ and $z_{R_{\max}}$ are not necessarily the same, leading to the need for a fixed reference point in this formulation. Finally, the sign and value of ζ_{ij} gives an immediate impression of how the plasma boundary curves in each quadrant.

3. Form for limited surfaces

With these definitions, it is now possible to proceed with the task of defining an analytic form that can reproduce boundaries like those shown in figures 1 and 2. It is convenient to start in this section with a form suitable for boundaries without x-points (like figure 1(a)). In the following section, this will be generalized to include the possibility of x-points at either or both extrema in the z direction.

Table 3. Values of the superellipse parameters in each quadrant in terms of the dimensionless geometric parameters.

Quadrant	x	y	A	B	n
I	$R + a(1/\varepsilon - \delta_u)$	$z - z_{off}$	$a(1 + \delta_u)$	$\kappa_u a$	$-\ln(2)/\ln[1/\sqrt{2} + \zeta_{uo}(1 - 1/\sqrt{2})]$
II	$a(1/\varepsilon - \delta_u) - R$	$z - z_{off}$	$a(1 - \delta_u)$	$\kappa_u a$	$-\ln(2)/\ln[1/\sqrt{2} + \zeta_{ui}(1 - 1/\sqrt{2})]$
III	$a(1/\varepsilon - \delta_l) - R$	$z_{off} - z$	$a(1 - \delta_l)$	$\kappa_l a$	$-\ln(2)/\ln[1/\sqrt{2} + \zeta_{u}(1 - 1/\sqrt{2})]$
IV	$R + a(1/\varepsilon - \delta_l)$	$z_{off} - z$	$a(1 + \delta_l)$	$\kappa_l a$	$-\ln(2)/\ln[1/\sqrt{2} + \zeta_{lo}(1 - 1/\sqrt{2})]$

The analytic form adopted here is that of the family of superellipses, also known as Lamé curves. The mathematical form is a straightforward generalization of equation (10):

$$(x/A)^n + (y/B)^n = 1, \tag{14}$$

where n is now a real number and $n > 1$ is used. The form of the superellipse conveniently allows each of the quadrants to be treated separately (i.e. A, B and n can have different values in each quadrant), while maintaining the property of being continuous and differentiable across all of the matching points ($x = 0$ or $y = 0$) since the limiting values of the derivative as these points are approached from opposite sides do not depend on the values of A, B or n.

For each quadrant, there are three unknowns (A, B, n) that must be determined from the geometrical constraints. The values of A and B have already been given in table 1 in terms of the extrema. Using equations (1) through (9), it is straightforward to transform these values into the dimensionless geometric quantities plus two dimensional quantities, which are chosen here to be a and z_{off}, without loss of generality (table 3). The value of n in each quadrant is determined uniquely by the value of ζ in that quadrant using the fact that point D in figure 2 must lie both on the curve determined by equation (14) and the line OE in figure 2 given by

$$y = (B/A)x. \tag{15}$$

Putting equation (15) into equation (14) and solving for the value of the intersection point D gives:

$$x_D = A/2^{1/n}, \tag{16}$$

or, solving for n:

$$n = -\ln(2)/\ln(x_D/A). \tag{17}$$

Using equation (11), it can be shown that

$$x_D = x_C + \zeta L_{CE}\cos(\phi), \tag{18}$$

where $\tan(\phi) = B/A$. After some algebra, equation (18) becomes:

$$x_D/A = 1/\sqrt{2} + \zeta(1 - 1/\sqrt{2}), \tag{19}$$

which uniquely determines n from the value of ζ (putting equation (19) into equation (17)). This form reinforces the interpretation of ζ as a measure of where the boundary is relative to the reference ellipse.

It is important to note that using the mathematical form of the superellipse limits the analytic form introduced here to generating curves that are everywhere convex, which implies that boundaries for indented plasmas and plasmas with higher order indentations such as so-called peapods cannot be generated with this form. While these shapes are of interest for theoretical studies, there are few present-day tokamaks that can make such shapes, and it is unlikely that plasmas for fusion energy production will have the coils necessary to generate them. Aside from the basic indentation, the capability of making such shapes is tied to the specific coil locations of a device, so it is difficult to envision a general analytic form to accommodate all conceivable coils, although it may be useful for theoretical studies to generate such forms. Despite this limitation, the form invoked here should suffice to generate the vast majority of plasmas of interest for experimental analysis and theoretical study.

4. Form for surfaces with x-points

The form introduced in the previous section was shown to be a suitable representation of a large variety of plasma shapes typical of experimental and theoretical studies. However, it is limited by design to boundaries that are everywhere continuous and differentiable. This eliminates a significant category of boundary shapes—those with a divertor configuration, i.e. an x-point where the magnetic field orthogonal to the direction of symmetry has a null. Fortunately, it is possible to extend the form introduced in the previous section to allow for an x-point at either or both of the extrema in the direction (the direction along the symmetry axis). In principle, the formulation could be extended to handle x-points at the extrema in the R direction (such as the polodial divertor implemented in JT-60).

To introduce a true x-point, the boundary at the extremum of interest must have the product of the slope of the boundary approaching the extremum on either side equal to -1. In the mathematical form of the superellipse introduced in the previous section (equation (14)), this is not possible since the slopes of the boundary approach from either direction asymptotically to 0. However, the form of the superellipse can be used if the minor and major axis values A and B are allowed to be variables, rather than defined by the extremum location (figure 3). To signify these are now variables instead of fixed quantities, the notation α and β will be used for the variable minor and major axes, respectively. This means that there are now three unknowns in each quadrant, requiring three constraints to define the values of α, β and n. Two of the constraints are easy to define: the x-point (X_x, y_x) and the point defined by the squareness (X_ζ, y_ζ) must lie on the boundary. It is important to remember that the coordinate X here is not that defined in table 1, because it now contains the variable α (table 4). The third constraint equation is given by defining

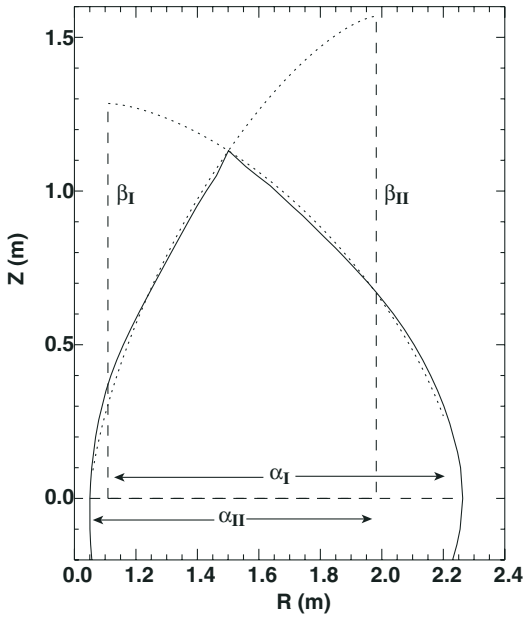

Figure 3. Example of how combining two superellipses with variable minor and major axes in both the inner and outer quadrants can reproduce an x-point plasma. The solid line is a reconstruction of a DIII-D plasma. The dotted lines are the super ellipse solutions in each quadrant. The dashed lines show the new minor (α) and major (β) axes found in quadrants I and II for the super ellipses. Note that the constraint of a perfect x-point (90° change in slope) is not satisfied in the reconstruction because it allows for a finite current density on the separatrix.

the slope of the line at the x-point. For example, in the upper outer quadrant, the following form is chosen:

$$\mathrm{d}y/\mathrm{d}X|_{X_x,y_x} = \begin{cases} \delta_u - 1, & \text{if } \delta_u \geqslant 0 \\ -1/(1+\delta_u), & \text{if } \delta_u < 0 \end{cases}. \qquad (20)$$

This definition for the slope reduces to the correct limits when $\delta_u = 1$, 0 or -1. While the limiting values of this slope constraint are correct, the functional form in between these limits is chosen for convenience, and a simultaneous solution to the three constraint equations is not guaranteed for arbitrary choices of the dimensionless geometric quantities defined in section 2. A better choice might be obtained by fitting a large database of boundaries derived from equilibrium reconstructions of actual experiments, but this has other difficulties and has not been attempted in the work reported here. The utility of this choice for the constraint will be demonstrated by examples in the following section.

The complete set of constraint equations to be solved for α, β and n in each quadrant is given in table 4. No analytic solution has been found for these three simultaneous equations. For the examples shown in the following section, a numerical solver employing the Newton method is used to determine the values α, β and n that satisfy the constraint equations in each quadrant.

5. Discussion

In the previous two sections, an analytic form has been introduced for generating potential boundary shapes without and with x-points. One test of the suitability of this form is to examine how well it can reproduce existing plasma shapes. A collection of comparisons between the boundary reconstructed from DIII-D plasmas and the boundary generated by the analytic form introduced above is shown in figure 4. The shape parameters used as input for the analytic form are those derived from the reconstructed boundary. It might be possible to minimize further the differences between the reconstructed boundary and the boundary generated by the analytic form by varying the input parameters slightly but that has not been attempted here. The two plasmas in the top row are limited plasmas where no x-point is present. For the low elongation case (figure 4(*a*)), it is difficult to see any difference between the reconstructed and analytic boundaries. For the high elongation case (figure 4(*b*)), the superellipse form does not quite reproduce the reconstructed plasma boundary near the top and bottom. The difference presents an illusion that the triangularity is not correctly determined, but the extrema and squareness constraints are satisfied. It is the functional form of the superellipse between these two points that does not match the reconstructed boundary. As mentioned above, this suggests that small variations in the squareness and triangularity in the analytic form would yield a more accurate reproduction on average; however, this would require development of a global measure of the goodness of fit. The power of the analytic form lies in the fact that it does a very good job of reducing the plasma shape to a small number of parameters without the need for fitting. The next example (figure 4(*c*)) adds x-points at both the top and bottom, plus illustrates the ability of the analytic form to handle significant up–down asymmetry. The analytic form lies outside the reconstructed boundary near the x-points, because the reconstruction allows for a finite (positive in this case) current density on the separatrix. In the lower inner quadrant, the superellipse form clearly matches the extrema and squareness constraint, but cannot reproduce exactly the reconstructed boundary, partly because the finite current density on the boundary appears to make the boundary slightly concave as it approaches the x-point. As mentioned above, the analytic form cannot reproduce a shape with concavity. But again, the overall match to the reconstructed boundary is quite good. The last example (figure 4(*d*)) is a quite extreme shape—very strong squareness with only slight up–down asymmetry. Again the analytic form fails to reproduce the concavity in the reconstructed boundary on the outboard side that arises from the finite spacing of the DIII-D poloidal field coils. But it does generally reproduce the boundary including an x-point at the bottom and none at the top, but with otherwise similar shapes. The overall conclusion from these examples is that the analytic form does a good job of capturing a large variety of plasma boundaries of interest.

Another test of the suitability of this form is the ease with which the boundary can be varied for physics studies. Two types of applications will be discussed here. First, one would often like to know the sensitivity of physics results such as MHD stability or transport to variations in shape. The analytic form introduced here allows generation of a family of solutions by varying only a single parameter. For example, starting from the form reproducing the ITER boundary from

Table 4. New variables and constraints for each quadrant for x-point plasmas.

Quadrant	X	x-point constraint	ζ-point constraint	x-point slope constraint
I	$R + a(1/\varepsilon - 1) - \alpha$	$[1 - a/\alpha(1 + \delta_u)]^n$ $+ (\kappa_u a/\beta)^n = 1$	$[1 + a(1 + \delta_u)(1 - 1/\sqrt{2})(\zeta_{uo} - 1)/\alpha]^n$ $+ (\kappa_u a[1/\sqrt{2} + \zeta_{uo}(1 - 1/\sqrt{2})]/\beta)^n = 1$	$\beta([\alpha - a(1 + \delta_u)]/\kappa_u a)^{n-1}$ $\times (\beta/\alpha)^{n-1} = \begin{cases} 1 - \delta_u & \delta_u \geqslant 0 \\ 1/(1 + \delta_u) & \delta_u < 0 \end{cases}$
II	$a(1/\varepsilon - 1) + \alpha - R$	$[1 - a/\alpha(1 - \delta_u)]^n$ $+ (\kappa_u a/\beta)^n = 1$	$[1 + a(1 + \delta_u)(1 - 1/\sqrt{2})(\zeta_{ui} - 1)/\alpha]^n$ $+ (\kappa_u a[1/\sqrt{2} + \zeta_{ui}(1 - 1/\sqrt{2})]/\beta)^n = 1$	$\beta([\alpha - a(1 + \delta_u)]/\kappa_u a)^{n-1}$ $\times (\beta/\alpha)^{n-1} = \begin{cases} 1/(1 - \delta_u) & \delta_u \geqslant 0 \\ 1 + \delta_u & \delta_u < 0 \end{cases}$
III	$a(1/\varepsilon - 1) + \alpha - Ra$	$[1 - a/\alpha(1 - \delta_l)]^n$ $+ (\kappa_l a/\beta)^n = 1$	$[1 + a(1 + \delta_l)(1 - 1/\sqrt{2})(\zeta_{li} - 1)/\alpha]^n$ $+ (\kappa_l a[1/\sqrt{2} + \zeta_{li}(1 - 1/\sqrt{2})]/\beta)^n = 1$	$\beta([\alpha - a(1 + \delta_l)]/\kappa_l a)^{n-1}$ $\times (\beta/\alpha)^{n-1} = \begin{cases} 1/(1 - \delta_l) & \delta_l \geqslant 0 \\ 1 + \delta_l & \delta_l < 0 \end{cases}$
IV	$R + a(1/\varepsilon - 1) - \alpha$	$[1 - a/\alpha(1 + \delta_l)]^n$ $+ (\kappa_l a/\beta)^n = 1$	$[1 + a(1 + \delta_l)(1 - 1/\sqrt{2})(\zeta_{lo} - 1)/\alpha]^n$ $+ (\kappa_l a[1/\sqrt{2} + \zeta_{lo}(1 - 1/\sqrt{2})]/\beta)^n = 1$	$\beta([\alpha - a(1 + \delta_i)]/\kappa_i a)^{n-1}$ $\times (\beta/\alpha)^{n-1} = \begin{cases} 1 - \delta_l & \delta_l \geqslant 0 \\ 1/(1 + \delta_l) & \delta_l < 0 \end{cases}$

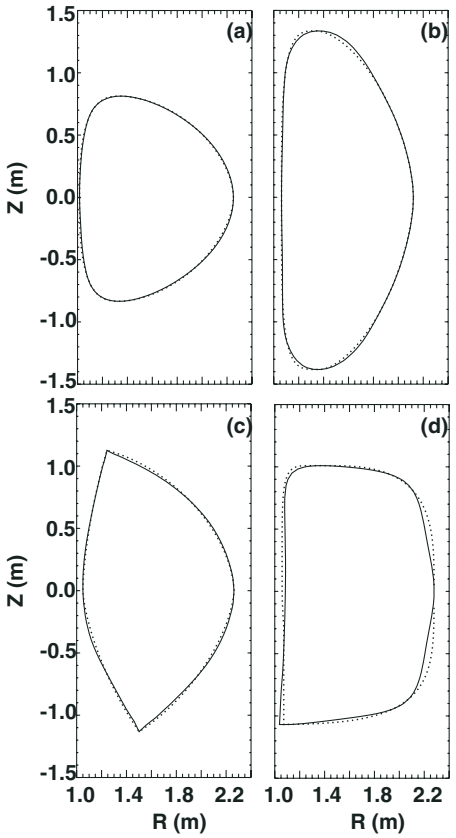

Figure 4. Examples comparing the boundary derived from a reconstruction of actual DIII-D plasmas (solid line) to that generated by the analytic form using the same geometric parameters (dotted line).

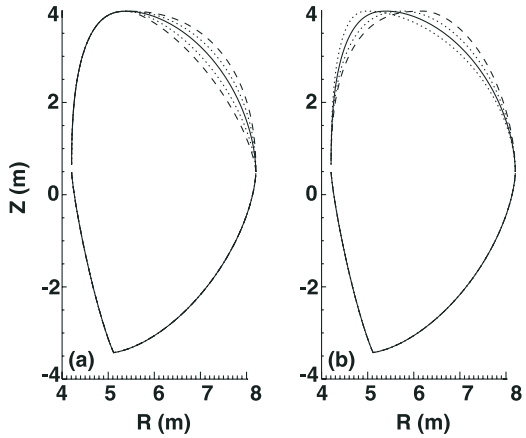

Figure 5. Variations about the ITER design shape in (a) upper outer squareness ζ_{uo} and (b) upper triangularity δ_u. In (a), the dotted and dashed curves outside the solid line correspond to an increase of 0.1 and 0.2 in ζ_{uo}, while the same line types inside the solid line correspond to an decrease of 0.1 and 0.2 in ζ_{uo}. In (b), the dotted line that extends outside the solid curve at the upper left represents an increase in δ_u of 0.2, while the dotted and dashed curves that extend outside the solid curve at the upper right represent a decrease in δ_u of 0.2 and 0.4, respectively.

figure 2, one can generate a series of boundaries where the upper outer squareness (figure 5(a)) or the upper triangularity (figure 5(b)) are changed, but the remaining shape parameters are fixed. These variations can then be used to generate equilibria for testing models; for example, models of pedestal stability, energy transport or the magnitude of fast ion ripple loss. Second, this form can be used to determine whether the coil currents required to make a desired shape that has not been made previously are within the capabilities of a given coil set. This is suggested by figure 4(d), where the general outline of the shape is defined by the analytic form, but the achieved shape requires a calculation with the actual poloidal field coil location and dimensions. For the studies in figure 5, there is theoretical interest in these variations about the ITER design shape, but there is also a practical interest in knowing whether the design poloidal field coil set is capable of supporting such variations. In figure 6, another example is shown where the question of whether a double-null divertor could be run in a circular cross-section machine by reversing the current in one set of coils is addressed. Providing target values of the poloidal field coil currents for the control system to use in generating a desired shape has significant practical value. The simple form for generating boundary shapes introduced here facilitates such an exercise.

In summary, a compact analytic form has been introduced that is capable of describing many axisymmetric plasma boundaries of interest in fusion research. Despite a long history of fixed boundary equilibrium calculations and describing

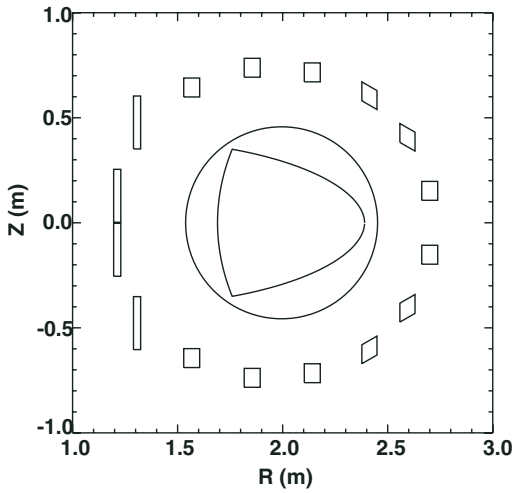

Figure 6. Example of a design shape for double-null operation within a coil set and limiter designed for circular limiter plasma operation. The specific coil and limiter locations in this example are from the RFX-Mod device.

reconstructed plasma boundaries by a reduced set of geometric parameters, no generally accepted analytic form that allows wide variation of parameters, up–down asymmetry and the possibility of x-points has been adopted. It is hoped that the utility of the form introduced here, as demonstrated by several examples, would lead to testing and eventual adoption of this form as a standard for future work. The geometric parameters defined extend those in standard use to allow a larger variety of shapes to be characterized for experimental work and generated for theoretical studies.

Acknowledgments

This work was supported by the US Department of Energy under cooperative agreement DE-FC02-04ER54698. The author is pleased to acknowledge discussions on shaping with J R Ferron, E A Lazarus and A D Turnbull that stimulated his interest in this work. The superellipse form for describing the plasma boundary was suggested by P A Politzer. The ITER boundary specification was provided by Y Gribov. The RFX-Mod coil set and limiter specifications were provided by the RFX-Mod team. Useful discussions with G Marchiori, P Martin and L Zanotto are gratefully acknowledged.

References

[1] Goldston R J 1984 *Plasma Phys. Control. Fusion* **26** 87
[2] Yushmanov P N *et al* 1990 *Nucl. Fusion* **30** 1999
[3] Troyon F *et al* 1984 *Plasma Phys. Control. Fusion* **26** 209
[4] Turnbull A D *et al* 1999 *Phys. Plasmas* **6** 1113
[5] Bulmer R H and Neilson G H 1997 *Proc. 17th Symp. on Fusion Engineering (San Diego, CA)* p 685
[6] Kotschenreuther M *et al* 2010 *Nucl. Fusion* **50** 035003
[7] Luxon J L 2002 *Nucl. Fusion* **42** 614
[8] Lao L L *et al* 1985 *Nucl. Fusion* **25** 1611
[9] Pomphrey N *et al* 1989 *Nucl. Fusion* **29** 465
[10] Cerfon A J and Freidberg J P 2010 *Phys. Plasmas* **17** 032502
[11] Leonard A W *et al* 2007 *Nucl. Fusion* **47** 552